Shear-wave-velocity drop prior to clayey mass movement in laboratory flume experiments

Article *in* Engineering Geology · April 2015

DOI: 10.1016/j.enggeo.2015.03.019

5 authors, including:

Guénolé Mainsant
University of Nantes
10 PUBLICATIONS **72** CITATIONS
SEE PROFILE

Guillaume Chambon
National Research Institute of Science and T…
92 PUBLICATIONS **507** CITATIONS
SEE PROFILE

Denis Jongmans
University Joseph Fourier - Grenoble 1
76 PUBLICATIONS **1,137** CITATIONS
SEE PROFILE

Eric Larose
French National Centre for Scientific Researc…
124 PUBLICATIONS **2,467** CITATIONS
SEE PROFILE

Engineering Geology 192 (2015) 26–32

Contents lists available at ScienceDirect

Engineering Geology

journal homepage: www.elsevier.com/locate/enggeo

Shear-wave-velocity drop prior to clayey mass movement in laboratory flume experiments

Guénolé Mainsant [a,b], Guillaume Chambon [c,d,*], Denis Jongmans [a,b], Eric Larose [a,b], Laurent Baillet [a,b]

[a] Univ. Grenoble Alpes, ISTerre, F-38041 Grenoble, France
[b] CNRS, ISTerre, F-38041 Grenoble, France
[c] IRSTEA, UR ETGR, Grenoble, France
[d] Univ. Grenoble Alpes, Grenoble, France

ARTICLE INFO

Article history:
Received 15 September 2014
Received in revised form 20 March 2015
Accepted 21 March 2015
Available online 3 April 2015

Keywords:
Clayey landslides
Trièves landslides
Flume experiment
Viscoplastic rheology
Acoustic monitoring
Wave-velocity drop

ABSTRACT

Clay slopes are susceptible to suddenly liquefy into rapidly accelerating landslides, thereby threatening people and facilities in mountainous areas. Because the shear-wave velocity (V_s) characterizes the medium stiffness, this parameter can potentially be used to investigate the rheological behavior of clay materials before and during the solid-to-fluid transition associated to such landslide failures. Previous rheometrical studies performed on clay samples coming from Trièves landslides (French Alps) have established that this material behaves as a yield stress fluid with a marked viscosity bifurcation. When the applied stress reaches a critical level, the viscosity decreases abruptly, along with V_s which tends to zero in the fully fluidized material. Here, we monitor the Rayleigh wave velocity (V_R) variations in a saturated clay layer placed in a flume and progressively brought to failure by tilting the device. Experiments performed on clay samples with different water contents show a significant relative drop in V_R values (and hence in V_s) before the onset of the mass movement. Additional rheometrical analyses point out that this precursory drop in V_s is presumably due to a complex transient rheological response of the clay. These new results confirm that V_s variations constitute a good indicator for monitoring clay slope stability.

1. Introduction

Clay landslides occur all over the world and represent a major threat to populations, due to their possible suddenness and their long runouts resulting from flow-like movements (van Asch and Malet, 2009). These landslides can involve volumes of millions of m^3 and reach longitudinal extensions of a few km, like the Slumgullion landslide (Colorado state; Gomberg et al., 2011), the Tessina landslide (Italy; Angeli et al., 2000), or the Maierato landslide (Italy; Gattinoni et al., 2012). The main hazards associated with these phenomena arise from the sudden acceleration of the clay slope and the unpredictable partial or total material fluidization that can occur during or after heavy and/or long-lasting rainfalls (Iverson et al., 1997; van Asch and Malet, 2009). This solid-to-fluid transition has been widely reported in numerous types of clayey deposits, including marine sensitive (Eilertsen et al., 2008) or non-sensitive clays (Picarelli et al., 2005; Gattinoni et al., 2012) and lacustrine clays (Bièvre et al., 2011). Flow-like movements have also been frequently observed in clay-rich rocks, like shales, marls and flyschs, which experience intense weathering and quick changes in rheology when sliding (e.g., Picarelli et al., 2005; van Asch and Malet, 2009; Piccinini et al., 2014).

The generation of flow-like movements (earth flows, debris flows) has been the subject of intense debate in the scientific community, with a long-lasting confrontation between elastoplastic and viscoplastic models (Iverson et al., 1997; Ancey, 2007). In elastoplastic models, predominantly used in soil mechanics, failure is generally governed by a frictional criterion, i.e. the yield strength surface is assumed to be linearly dependent on the average normal stress. Soil fluidization is then generally related to an increase in pore water pressure which can produce a state of zero effective normal stress in the soil mass (Iverson et al., 1997; Iverson, 2005b). Viscoplastic models, proposed by the fluid-mechanics community, assume that soil can flow when shear stresses exceed a yield shear strength which is considered as an intrinsic property of the material at a given water content (Ancey, 2007).

Numerous laboratory experiments performed on water-clay dispersions demonstrated the potential of viscoplastic models for explaining the rheological behavior of homogenized fine-grained materials (Coussot et al., 1998; Ancey, 2007; Jeong, 2013). In particular, it was shown that increasing the fine-fraction content in a coarse-grained suspension provokes a change in rheology, from a frictional to a viscoplastic regime (Coussot and Ancey, 1999). However, in poorly sorted materials, results show that the bulk rheology can obey either frictional or viscoplastic models, while the flow properties also depend on the flow organization, lateral levées segregation and entrainment processes (Iverson, 2005a; Iverson et al., 2011; Johnson et al., 2012; Quan Luna et al., 2012).

* Corresponding author at: IRSTEA, UR ETGR, Grenoble, France.
E-mail address: guillaume.chambon@irstea.fr (G. Chambon).

http://dx.doi.org/10.1016/j.enggeo.2015.03.019
0013-7952/

The rheology of fine-grained materials is then often described according to viscoplastic laws, such as the Herschel–Bulkley model (Coussot et al., 1998; Huang and Garcia, 1998), for which, in simple shear, flow is possible only above a critical yield stress τ_c:

$$\begin{cases} \tau \le \tau_c; & \dot{\gamma} = 0 \\ \tau > \tau_c; & \tau = \tau_c + K\dot{\gamma}^n \end{cases} \quad (1)$$

where τ is the shear stress, $\dot{\gamma}$ is the shear strain rate, and K and n are two additional material parameters. For an inclined soil layer of thickness h overlying a rigid substratum, the shear stress at the layer bottom is given by:

$$\tau = \rho g h \sin\theta \quad (2)$$

where θ is the inclination angle, ρ is the material density and g is the gravity acceleration. When the shear stress τ exceeds τ_c (which can occur by increasing either θ or h), the material starts flowing. Certain clays, such as bentonite (Coussot et al., 2002; Ovarlez et al., 2009) or quick clays (Khaldoun et al., 2009), are also characterized by thixotropy (time-dependent behavior) and abrupt viscosity bifurcations. For stress levels smaller than τ_c, transient creep is possible during which the apparent viscosity of the material continuously increases until complete cessation of flow. Above the critical stress, on the contrary, the viscosity abruptly decreases and flow rapidly develops. Recently, such a thixotropic behavior, with a pronounced viscosity bifurcation, has been observed on clay materials sampled from Trièves landslides (French Alps) for water contents exceeding the liquidity limit (Mainsant et al., 2012a), and might explain the occurrence of sudden fluidization events in the field.

The viscoplastic and/or thixotropic properties of materials can be determined from laboratory rheometer tests (Coussot et al., 1998; Bardou et al., 2007). However, no direct measurements of the rheological properties are possible in the field, and testing these properties on samples collected in situ remains a difficult task, due to the usually broad particle size distribution in natural flows (Ancey, 2007; Bardou et al., 2007). Finding indirect markers of the rheological processes leading to the solid-to-fluid transition would therefore be of great interest for operational applications. Previous field and laboratory studies on Trièves clay have shown that the shear-wave velocity V_s could constitute such a proxy (Jongmans et al., 2009; Renalier et al., 2010). Recent oscillatory rheometrical tests performed on this material showed that the linear elastic shear modulus G, which is directly related to V_s, undergoes a marked drop concomitant with the viscosity bifurcation observed at the critical stress (Mainsant et al., 2012a). Consistently, in the field, passive seismic monitoring of the Pont Bourquin landslide (Switzerland) showed a 45% drop in V_s (from 360 to 200 $m \cdot s^{-1}$) at the base of the landslide a few days before the occurrence of an earthflow (Mainsant et al., 2012b).

All these results suggest that V_s might constitute a good marker for the solid-to-fluid transition in clay materials, and could even be used as a precursor for the prediction of fluidization events. However, the repeatability of the precursory drop in V_s, as well as its physical origin, needs to be investigated and better understood. This paper reports on the results of laboratory flume experiments and rheometrical tests specifically designed to that purpose. The flume was filled with water-saturated Trièves clay and progressively tilted until failure. The Rayleigh wave velocity V_R in the material was continuously monitored and compared to displacement measurements. As will be shown, these experiments offered us the possibility to follow wave velocity variations in a model slope progressively brought to failure under well-controlled conditions, and to confirm the predictive capabilities of V_s. In parallel, rheometrical tests were used to determine the rheological properties of the clay samples. A specific protocol was designed to provide insight in the evolution over time of the elastic shear modulus G of samples submitted to constant loading. These tests suggest that precursory drops in V_s could be related to a complex transient rheological response of the material.

2. Flume experiments

2.1. Experimental device

The setup of the inclined plane experiment is shown in Fig. 1a and b. The flume has transparent sides and is 1 m long, 0.3 m wide and 0.3 m high. It is embedded on a metallic frame and its tilt angle is controlled by a step motor. The used clay material was sampled in a gully of the

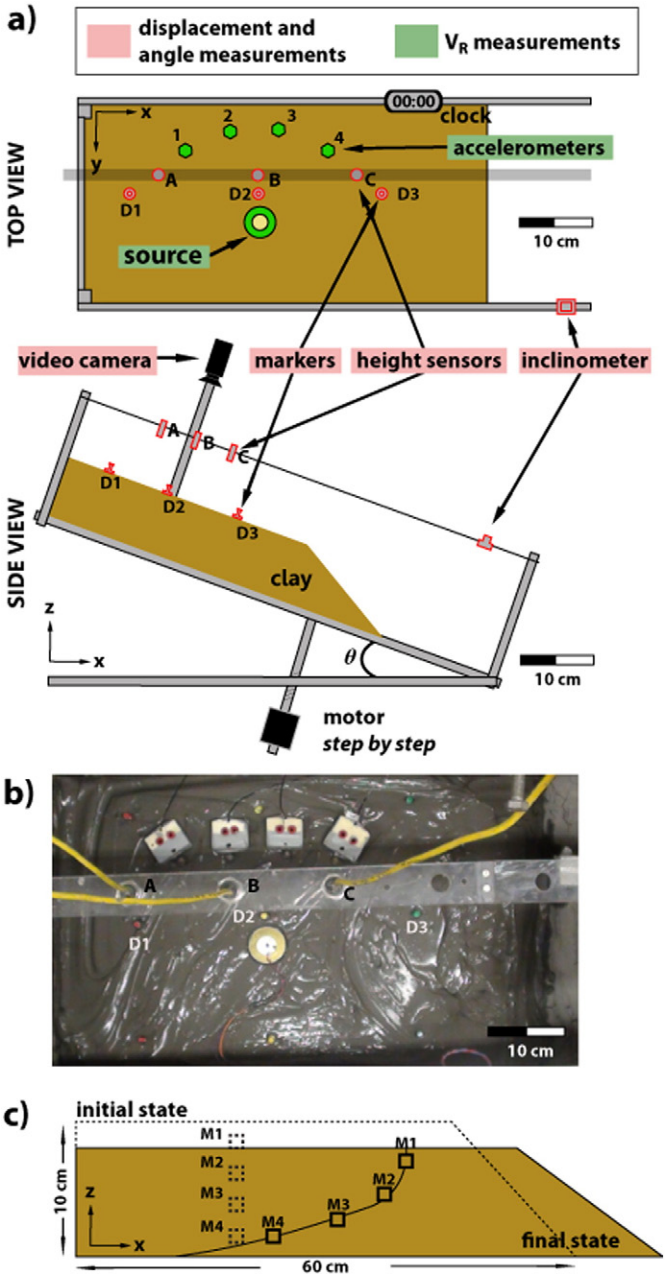

Fig. 1. (a) Sketch of the flume setup (top and side views), with the different measurement devices (θ denotes the flume tilt angle). Acoustic and displacement measurement devices are indicated in green and pink, respectively. D1 to D3: thumbtacks. (b) Picture (top view) of the experiment. (c) Geometry of the clay mass at the initial and final states. The solid and dotted rectangles represent 4 plastic markers (numbered from M1 to M4) and illustrate the typical displacement profile observed within the layer.

Trièves plateau, located between the two landslides of Avignonet and Harmalière (Bièvre et al., 2011). The geotechnical properties of the glaciolacustrine clays found in the Trièves area have been documented in previous studies (Giraud et al., 1991). The main minerals are illite (42–47%), calcite (15–20%), quartz (14–16%), chlorite (14–16%), and feldspar (5–10%). Consolidated drained direct shear tests provided residual values of practically zero for the cohesion and of 18–19° for the friction angle. In addition, Atterberg limits were measured and grain size analysis was performed on 3 of the samples used in this study. The soil presents 96–100% by weight of fines passing the #200 sieve (0.075 mm), and a LL (resp. IP) value of 0.44 (resp. 0.2) was obtained. According to the Unified Soil Classification System (USCS), the soil is classified as CL (clay of low plasticity).

Samples of different concentrations were prepared by mixing the clay material with water. Since the mechanical behavior of clay dispersions is known to be sensitive to water ionic content (Anson and Hawkins, 1998), the water used for the preparation of the samples came directly from the field, from a piezometer installed at the Avignonet landslide. Note that fixing a priori the gravimetric water content w (ratio of water to solid mass) of the samples turned out to be difficult, due to evaporation and material loss during the mixing phase. Consequently, w was measured a posteriori by drying and weighing the samples. These remolded samples were then placed manually in the initially horizontal flume, to form 55 cm-long and 10 cm-thick layers with a downward-sloping edge (Fig. 1a). The setup was left to rest for 2 h after the preparation, before starting to tilt the flume at a constant rate of 1°/min. This tilting rate was chosen sufficiently low to assume quasi-static loading conditions, but large enough to prevent drying of the samples during the experiments. Temperature and humidity were constant during the short experimental duration (less than 30 min). The flume tilt angle was measured by a digital inclinometer (CXTA01) with an accuracy of 0.03°.

A digital camera placed above the flume continuously monitored the experiments. Three surface markers (thumbtacks D1 to D3 in Fig. 1a) were followed on the images with an accuracy of about 0.2 cm, using Avimeca software (www.discip.ac-caen.fr/phch/labo/labo.htm). In complement, surface displacements were also assessed through three ultrasonic height sensors (Banner, type Q45UR) placed 15 cm above the sample. These sensors (A, B, C in Fig. 1a) provided measurements of the thickness variations of the clay layer, with a relative accuracy of 0.4%. Lastly, the Rayleigh wave velocity V_R in the material was monitored using a 5 cm-piezoelectric source (Kingstate KPS-100) placed at the surface, in the center of the clay mass, and four vertical accelerometers (Bruel&Kjæ, type r 4393V) installed on the side of the sample, at about 15 cm from the source. The accelerometers were mounted on small polystyrene blocks "floating" in the saturated clay. The source generated a 1 s-long chirp signal with frequencies ranging from 100 Hz to 600 Hz. The recorded signals were correlated with the source to reconstruct the Rayleigh wave propagation (see Larose et al., 2007, for more details), and the Rayleigh velocity V_R was derived by picking the maximum of the signal envelopes. The maximum Rayleigh wavelength, obtained in an experiment with $V_R \approx 12\ \mathrm{m\cdot s^{-1}}$, varies between 2 cm and 12 cm in the generated frequency range. Hence, the corresponding maximum penetration depth, approximately defined by half the wavelength (6 cm) (Park et al., 1999), is always smaller than the thickness of the sample. Under this condition, the Rayleigh velocity V_R can be regarded as directly proportional to the shear wave velocity V_s of the material (Viktorov, 1967). The respective positions of the source and receivers were followed on the camera images, and the wave velocities were corrected for distance variations. The absolute errors on V_R values were estimated to be about $0.2\ \mathrm{m\cdot s^{-1}}$.

2.2. Results

Preliminary experiments were performed to investigate the displacement field within the clay mass upon the occurrence of failure. Four small plastic markers ($1\ \mathrm{cm^3}$) were initially placed along a vertical profile within the sample (M1, M2, M3, M4; Fig. 1c). The flume was then progressively tilted, and the experiment was stopped when the extremity of the clay mass reached the bottom of the flume. Sketches of the initial and final geometry of the clay volume are shown in Fig. 1c. The final marker positions indicate that the total shear deformation remains small in the upper part of the layer and is maximal at the base. This type of displacement profile, with a sheared layer at the base and a plug at the top, is in good agreement with the typical behavior expected for a viscoplastic material in a free-surface flow (Coussot, 1994; Chambon et al., 2014).

The results of two typical experiments with different gravimetric water contents w are presented in Figs. 2 ($w = 0.57$) and 3 ($w = 0.68$). For $w = 0.57$, the Rayleigh-wave velocity V_R is observed to remain constant, at a value of $12.2\ \mathrm{m\cdot s^{-1}}$, until the tilt angle reaches $\theta_1 = 8°$ (time t_1 in Fig. 2b). During this period, no displacement is recorded by the height sensors (Fig. 2c) and the displacement markers (Fig. 2d). At time t_1, V_R starts to decrease. However, the first significant surface displacements are detected only at $t_2 > t_1$, for a tilt angle $\theta_2 = 14°$. At this time, V_R has already dropped by about 4% and continues to follow the same trend. From t_2 on, the thickness variations and surface displacements show a progressive, exponential-like, acceleration until

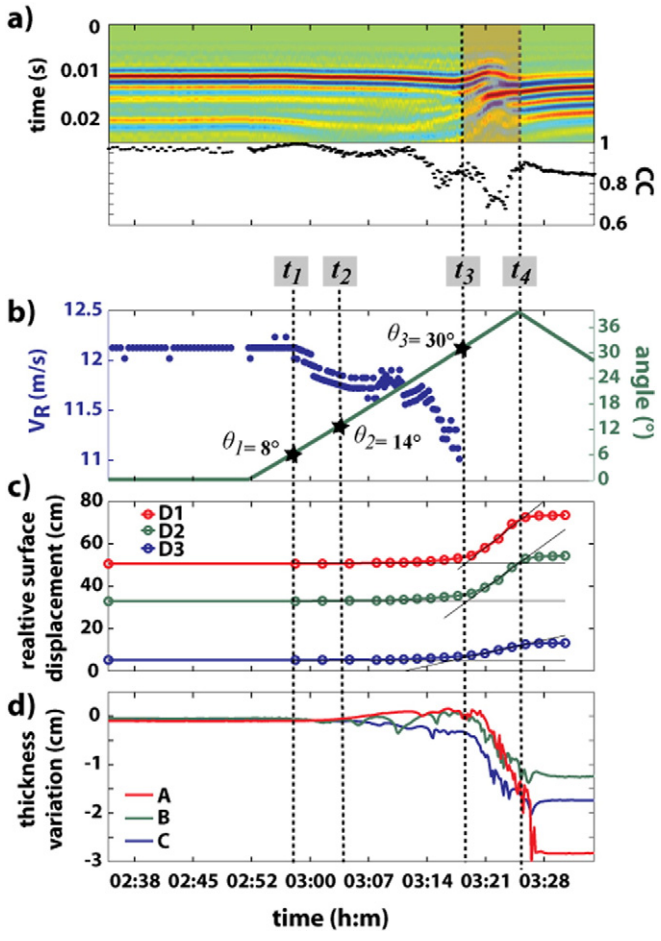

Fig. 2. Results of flume experiment for a water content $w = 0.57$. (a) Rayleigh wave correlogram and corresponding correlation coefficient *CC*. The time-period marked by important changes in waveform, during which V_R measurements cannot be performed, is indicated by darker colors. (b) Rayleigh wave velocity V_R (blue) and tilt angle θ (green). (c) Positions of the three surface markers (D1 to D3), measured relatively to the top end of the sample. (d) Thickness variations measured by the three ultrasonic height sensors (A to C). The time axis is common to all plots. The different characteristic times t_1 to t_4 (see text) were determined by visual inspection of the curves.

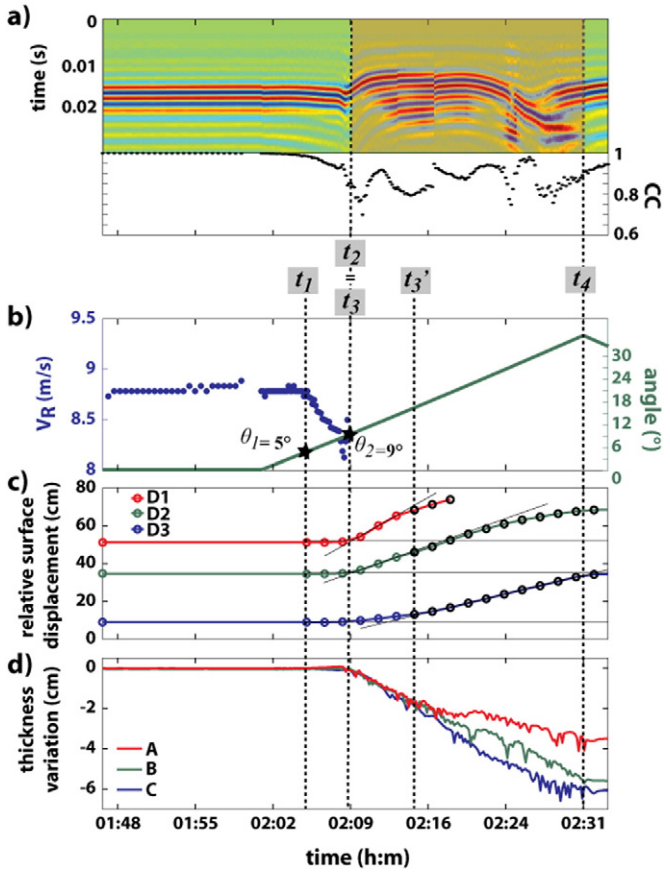

Fig. 3. Results of flume experiment for a water content $w = 0.68$. (a) Rayleigh wave correlogram and corresponding correlation coefficient *CC*. The time-period marked by important changes in waveform, during which V_R measurements cannot be performed, is indicated by darker colors. (b) Rayleigh wave velocity V_R (blue) and tilt angle θ (green). (c) Positions of the three surface markers (D1 to D3), measured relatively to the top end of the sample. (d) Thickness variations measured by the three ultrasonic height sensors (A to C). The time axis is common to all plots. The different characteristic times t_1 to t_4 (see text) were determined by visual inspection of the curves.

reaching time t_3 (corresponding to a tilt angle $\theta_3 = 30°$ and a total decrease in V_R of 7%), at which surface velocities stabilize around values exceeding 0.5 cm·min^{-1}. The surface velocities then remain quasi-constant until the flume tilting is eventually stopped at time t_4. This constant-velocity flow results in significant perturbations of the medium, as shown by the wave correlogram and the degradation of the correlation coefficient, whose value falls below 0.8 at t_3 (Fig. 2a). As a consequence, reliable V_R values can no longer be obtained for $t > t_3$. Finally, surface displacements immediately stop when the tilt angle starts to be reduced at time t_4.

With a higher water content, namely $w = 0.68$ (Fig. 3), the initial value of the Rayleigh-wave velocity, $V_R = 8.7$ m·s^{-1}, is lower. This result is consistent with the decrease of V_s with w reported in laboratory tests by Mainsant et al. (2012a). However, the general pattern of signal evolutions is similar to that observed for $w = 0.57$. The velocity V_R starts to decrease when the flume angle reaches $\theta_1 = 5°$ (Fig. 3b), whereas significant surface displacement and thickness variations become visible only for a larger tilt angle: $\theta_2 = 9°$ (Fig. 3c and d). Between these two angle values, V_R drops by about 7%. The transient, accelerating phase detected for $w = 0.57$ is not observed in this case, and surface velocities quasi-immediately reach constant values that exceed 0.5 cm·min^{-1}. The wave correlogram is again strongly perturbed, preventing accurate determinations of V_R to be obtained. At time t_3', the flowing material reaches the bottom of the flume, which further disrupts the experiment results before reaching the maximum tilt angle (time t_4).

3. Rheometrical tests

3.1. Testing protocol

To gain more insight into the results obtained in the flume experiments, the clay samples have been subjected to laboratory rheometrical tests aiming at characterizing the mechanical behavior of the material in the vicinity of the solid-to-fluid transition. Two types of loading protocols were applied (Fig. 4). Standard creep tests similar to those described in Mainsant et al. (2012a), consisting in monitoring the evolution of the shear strain rate $\dot{\gamma}$ under constant imposed levels of shear stress τ, were used to determine the values of the critical yield stress τ_c and to follow the changes in apparent viscosity $\eta_a = \tau/\dot{\gamma}$ over time (Fig. 4b). In addition, specific tests have been designed to capture the evolution of the elastic shear modulus G during these creep phases. The protocol consisted in superimposing small stress oscillations over a constant mean stress level τ, and monitoring the resulting response in shear strain (Fig. 4c). As for the standard creep tests, different levels of mean stress, ranging from below to above the yield stress, were investigated. The amplitude and frequency of the superimposed oscillations were kept constant, equal to 10 Pa and 5 Hz respectively. These values were chosen to (1) ensure a linear response of the material, and (2) be in a regime where the viscoelastic storage modulus (Bird et al., 1987) is independent of the frequency and well-representative of the elastic shear modulus G. Compared to previously reported results, for which only the steady state values of the shear modulus were monitored (Mainsant et al., 2012a), this new protocol allowed us to follow the transient response of G when a given load is applied. Combination of these two types of creep tests thus provides information on the evolutions over time of both η_a and G in the vicinity of the solid-to-fluid transition.

As mentioned previously, due to difficulties (homogenization, evaporation) involved in the material preparation, it was not possible to obtain samples at a predetermined water content w. Therefore, the two types of rheometrical tests were performed on samples with close, but slightly different, values of w. Before each experiment, the samples were pre-sheared at a strain rate of 50 s^{-1} during 10 s, and then left at rest for 10 s, in order to ensure a reproducible initial state.

3.2. Results

Fig. 5 presents typical results of the rheometrical tests for three different water contents w. First, and consistently with the previous results of Mainsant et al. (2012a), standard creep tests reveal a viscoplastic rheological behavior marked by clear viscosity bifurcation at the solid-to-fluid transition. In particular, the large-time values of apparent viscosity η_a display an abrupt drop when the yield stress τ_c is reached (Fig. 5d to f). Still consistently with previous results, oscillatory tests show that the large-time values of elastic shear modulus G also undergo a marked drop at a critical level of stress (Fig. 5a to c). The slight differences in sample water contents w prevent direct comparisons between the two types of tests. However, the empirical correlation between τ_c and w established by Mainsant et al. (2012a) can be used to ascertain that, within experimental uncertainty, the critical stress level for G is identical to the yield stress at which the viscosity bifurcation occurs.

It can also be observed in Fig. 5 that, both below and above the yield stress τ_c, the steady-state levels in η_a and G are reached after relatively long transient phases. The duration of these transients varies from a few seconds to several tens of seconds, and appears to be longer in the vicinity of the yield stress. For $\tau < \tau_c$, η_a and G display increasing trends, starting from relatively low values (compared to the final steady-state levels). For $\tau > \tau_c$, and except for the lowest water content (Fig. 5a and d), η_a and G pass through an initial peak before decreasing and progressively leveling out at their final steady state values (Fig. 5b, c and e, f).

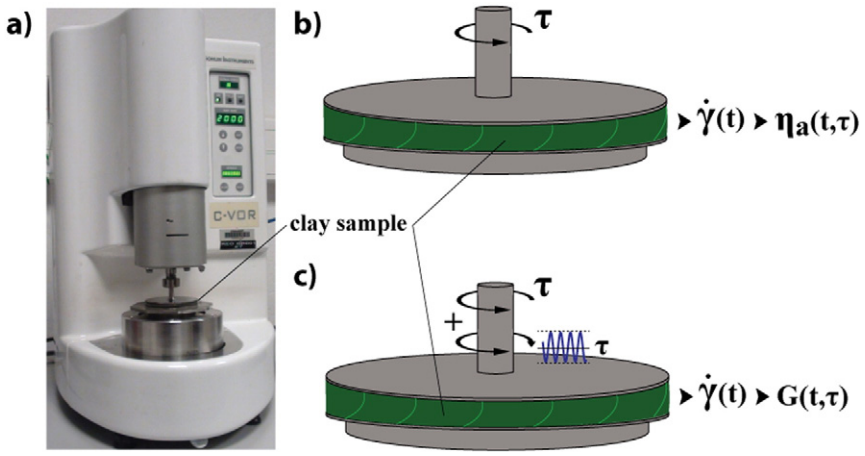

Fig. 4. (a) Laboratory stress-controlled rheometer used in this study (Bohlin-CVOR). (b) and (c) Schematic representation of the two types of rheometrical tests performed: standard creep tests to determine the material apparent viscosity η_a (b) and creep tests with superimposed stress oscillations to determine the elastic shear modulus G (c). See text for additional details.

This phenomenon could be described as a delayed fluidization of the material, and is particularly marked close to the yield stress. The existence of these time-dependent responses is a clear hallmark of the thixotropic behavior of the studied clay. Interestingly, the data also seem to indicate that the duration of the transients, and in particular of the delayed fluidization phases, is generally longer for the apparent viscosity η_a than for the elastic shear modulus G. For example, for the highest water contents, transient variations in η_a lasting more than 200 s are observed in the vicinity of the yield stress (Fig. 5f), whereas the values of G stabilize in less than 30 s (Fig. 5c). This result could be interpreted as the existence of several different microstructural response times in the clay material. Additional and more systematic experimental campaigns, which lie beyond the scope of this preliminary study, would nevertheless be needed to confirm this observation.

4. Discussion

In Fig. 6a, the two flume experiments described above are compared by converting the tilt angle θ into a shear stress representative of the loading applied at the base of the clay layer, using Eq. (2). Three characteristic stress levels, corresponding to the particular tilt angles θ_1, θ_2 and θ_3 defined in Section 2.2, are introduced: $\tau_{V_R} = \rho g h \sin\theta_1$ is the stress at

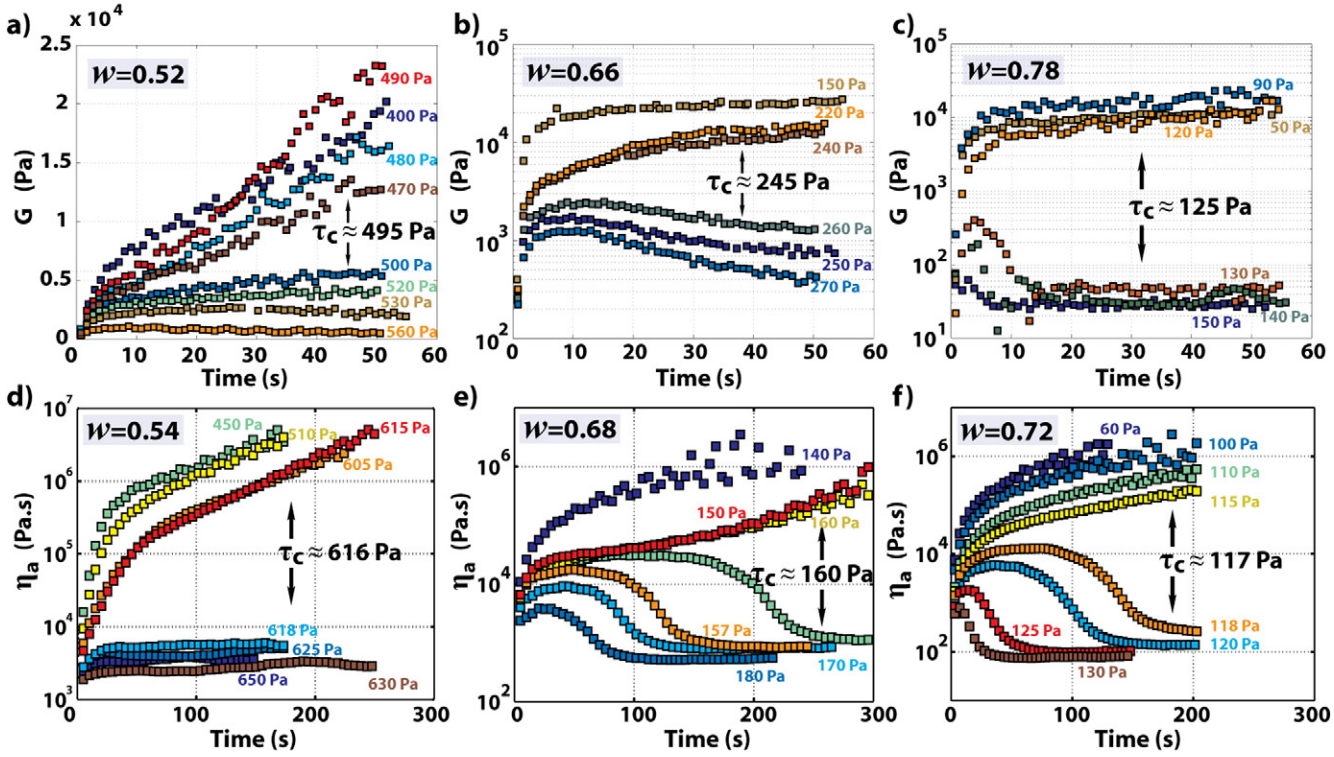

Fig. 5. Variations of the elastic shear modulus G (a, b, c) and the apparent viscosity η_a (d, e, f) during creep tests for different levels of imposed shear stress τ and different water contents w (indicated in legend). The quantities η_a and G are measured using distinct experimental protocols, and hence could not be obtained for exactly identical water contents (see text).

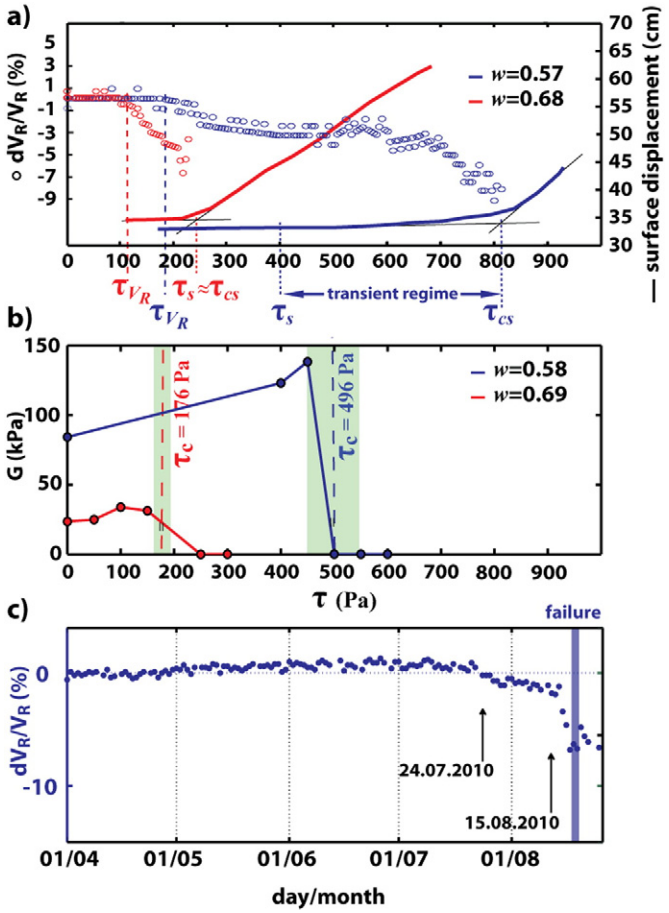

Fig. 6. (a) Relative variations in Rayleigh wave velocity V_R (circles) and surface displacements for marker 2 (lines) measured in the flume experiments as a function of the calculated shear stress τ, for the two water content values w. The characteristic stress levels τ_{V_R}, τ_s and τ_{cs} are defined in text. (b) Synthetic results of rheometrical tests for quasi-identical water contents: values of yield stress τ_c and variations of the steady-state elastic shear modulus G as a function of the applied shear stress (see Mainsant et al., 2012a, for more details on these tests). The green domains represent the uncertainties on the measured τ_c-values. (c) Relative variations in V_R as a function of time measured through passive seismic monitoring at the Pont Bourquin landslide before the occurrence of a fluidization event (vertical blue line) (Mainsant et al., 2012b).

which the Rayleigh wave velocity V_R starts to drop, $\tau_s = \rho g h \sin\theta_2$ is the stress required to initiate discernible surface movements in the clay mass, and $\tau_{cs} = \rho g h \sin\theta_3$ is the stress for which the constant-velocity flow regime is reached. These stress estimates were computed considering the initial thickness of the soil samples, $h = 10$ cm.

The main result of the flume experiments is that, for all the water contents investigated, τ_{V_R} is systematically and significantly smaller than τ_s (Fig. 6a). These laboratory experiments thus confirm the possibility to observe variations in V_R, and hence in shear-wave velocity V_s, which constitute precursors for the initiation of the mass movement. For the case $w = 0.68$, $\tau_{V_R} \approx 110$ Pa whereas $\tau_s \approx 240$ Pa. For $w = 0.57$, the difference between $\tau_{V_R} \approx 180$ Pa and $\tau_s \approx 400$ Pa is even larger. Let us also emphasize that the total relative decrease in V_R observed at the onset of clay displacement (7% and 4% for $w = 0.68$ and 0.57, respectively) is always higher than the estimated experimental errors (which are less than 2.5%).

The stress levels inferred from the flume experiments can also be compared to the critical yield stress τ_c determined in the rheometrical tests (Fig. 6b). Creep tests performed for similar water contents, namely $w = 0.69$ and 0.58, provided τ_c-values of 176 Pa and 496 Pa, respectively (Mainsant et al., 2012a). For the higher water content, τ_c is therefore comprised between the stress levels τ_{V_R} and τ_s corresponding to the onset of wave velocity drop and the initiation of clay movement. For the lower water content, τ_c is slightly larger than τ_s, but significantly lower than the stress level τ_{cs} for which the constant-velocity flow regime is reached (Fig. 6a). Globally, it can thus be concluded that the solid-to-fluid transition in the flume, be it either defined as the first drop in V_R or as the initiation of surface movements, occurs for stress levels which are on the same order as the yield stress τ_c of the clay, as expected for a viscoplastic material. However, due to the various sources of uncertainties, it is not possible at this stage to conclude whether or not τ_c could be unambiguously identified with either τ_{V_R} or τ_s, or whether τ_c systematically lies between these two stress levels. These uncertainties arise from (1) the experimental errors and variability involved in the rheometrical tests (Mainsant et al., 2012a), (2) the difficulties in precisely controlling the water content of the samples, and (3) the estimates of the shear stress in the flume using Eq. (2) which disregard, in particular, the effects of friction along the side walls.

It shall nevertheless be emphasized that, in the rheometrical tests, the stress level required to trigger the significant drop in G (and then in V_s) is the same as the stress level at which the viscosity bifurcation, and hence flow initiation, occurs. This result appears to be conflicting with the difference between τ_{V_R} and τ_s, and the precursory variations in V_R, observed in the flume experiments. Elaborating on the preliminary data presented in Section 3.2 which suggest that, in the vicinity of the solid-to-fluid transition, the transient variations in elastic modulus G occur over shorter response times than the transient variations in apparent viscosity η_a, we argue that this apparent contradiction could be explained by the time-dependent behavior of the clay. More specifically, we recall that, unlike the rheometrical tests which are performed at constant stress levels, flume experiments involve a continuous increase of the tilt angle, i.e. a continuous increase of the load applied to the samples. The precursory variations in V_R could then be related to transient phases of delayed fluidization during which, given the applied loading rate, the modulus G has enough time to drop to its "fluid" level whereas the apparent viscosity η_a remains very high, thereby impeding flow initiation. This interpretation implies that the two characteristic stress levels τ_{V_R} and τ_s determined in the flume experiments should progressively converge, and become identical to the rheometrical yield stress τ_c, when the loading rate is reduced. The validity of this prediction, and more generally the role of the thixotropic behavior of the clay on the precursory V_R-changes, will need to be investigated further through experiments involving different loading protocols, e.g. reducing the flume tilting rate or imposing tilt angle plateaus (not possible with the present setup).

Lastly, it is interesting to compare the results of these flume experiments to the relative variations in V_R measured at the Pont-Bourquin landslide just before the occurrence of an earthslide/earthflow on August 18, 2010 (Mainsant et al., 2012b). This small but active landslide, located 20 km east of Geneva Lake in the Swiss Prealps, is 240 m long and 15–60 m wide. Its depth, estimated from seismic imaging and electrical tomography, is about 11 m. The sliding material is predominantly clayey, composed of a mixture of moraine material, principally in the upper part, and debris from Aalenian black shales, flysch sandstones and marl alternations (Jaboyedoff et al., 2009). The monitoring performed in 2010 revealed that the water table rose from −4 m to −1 m depth before occurrence of the earthflow (Mainsant et al., 2012b). As shown in Fig. 6c, the wave velocity V_R remained almost stable during the whole spring, and started to decay 20 days before the failure. A decrease of 2% in V_R was observed between July 24 and August 15, preceding a larger drop of 5% that occurred three days before the earthflow. Interestingly, these wave velocity variations appear to be in the same range (7–9%) as those observed in the flume experiments (Fig. 6a). Moreover, the changes in V_R measured in the flume for $w = 0.57$ show a trend very similar to that observed at Pont Bourquin, with a first gentle velocity decrease of about 2%, then followed by an abrupt drop before failure (Fig. 2b). The seismic study at Pont Bourquin,

with the input of geotechnical data, showed that the measured decay in V_R resulted from a 45% drop in V_s (from 360 to 200 $m \cdot s^{-1}$) in a 2 m thick zone located at the base of the landslide (Mainsant et al., 2012b). The similarity between the shear deformation patterns observed in the flume experiments (Fig. 1c) and at Pont Bourquin suggests that the V_R decrease measured in the laboratory could also result from a drastic drop in V_s at the base of the clay layer.

Clearly, this comparison between laboratory and field results remains purely qualitative at this stage, since the flume tests were not designed as a physical model of the Pont Bourquin landslide. However, the striking similarities observed seem to indicate that the changes in V_R observed at Pont Bourquin are effectively related to the solid-to-fluid transition undergone by the clay. Furthermore, as in the laboratory tests, the precursory drop in V_R (and V_s) observed prior to failure is presumably due to complex transient rheological effects in the material when the stress state approaches the critical yield envelope.

5. Conclusions

The laboratory experiments performed in this study allowed us to model the initiation and fluidization of small-scale clayey landslides under well-controlled conditions. The mass movements were initiated by a progressive increase of the slope angle and eventually developed into constant-velocity flows, with a maximum shear rate at the base. Through a continuous monitoring of acoustic-wave velocity in the material, we demonstrated the existence of systematic precursory drops in shear-wave velocity which occur prior to the onset of discernible movements. Original rheometrical tests (creep tests with superimposed oscillations to monitor the evolution of the elastic shear modulus) were used to understand the physical origin of this phenomenon. We hypothesize that the precursory wave-velocity drops are caused by a complex transient rheological response of the clay samples, with the existence of "delayed fluidization" phases during which the shear modulus of the material rapidly drops while the apparent viscosity evolves more slowly and needs more time to reach its fluid level. Interestingly, the evolution of shear-wave velocity in the experiments was shown to follow a trend very similar as that observed in the field, prior to the occurrence of a real earthflow. The experimental study presented in this paper thus confirms that the shear-wave velocity V_s represents a relevant proxy for the monitoring of fluidization in clayey slopes, and opens up promising prospects for the definition of V_s thresholds in operational early warning and alert systems.

Acknowledgments

The authors thank Frederic Ousset and Christian Eymond-Gris from IRSTEA, and Julien Turpin from ISTerre, for their help with the installation of the experimental set-up. The authors also acknowledge financial support from the French ANR project SISCA (ANR-08-RISK-009), and from the VOR federative structure. This work is part of the Labex OSUG@2020 (Investissements d'Avenir — grant agreement ANR-10-LABX-0056).

References

Ancey, C., 2007. Plasticity and geophysical flows: a review. J. Non-Newtonian Fluid Mech. 142, 4–35.
Angeli, M.G., Pasuto, A., Silvano, S., 2000. A critical review of landslide monitoring experiences. Eng. Geol. 55 (3), 133–147.
Anson, R.W.W., Hawkins, A.B., 1998. The effect of calcium ions in pore water on the residual shear strength of kaolinite and sodium montmorillonite. Geotechnique 48 (6), 787–800.
Bardou, E., Bowen, P., Boivin, P., Banfill, P., 2007. Impact of small amounts of swelling clays on the physical properties of debris-flow-like granular materials. Implications for the study of alpine debris flow. Earth Surf. Process. Landf. 32 (5), 698–710.
Bièvre, G., Kniess, U., Jongmans, D., Pathier, E., Schwartz, S., van Westen, C., Villemin, T., Zumbo, V., 2011. Paleotopographic control of landslides in lacustrine deposits (trièves plateau, french western alps). Geomorphology 125, 214–224.
Bird, R.B., Armstrong, R.C., Hassager, O., 1987. Dynamics of Polymeric Liquids. second edition. Fluid Mechanics vol. 1. Wiley-Interscience.
Chambon, G., Ghemmour, A., Naaim, M., 2014. Experimental investigation of viscoplastic free-surface flows in steady uniform regime. J. Fluid Mech. 754, 332–364.
Coussot, P., 1994. Steady, laminar, flow of concentrated mud suspensions in open channel. J. Hydraul. Res. 32 (4), 535–559.
Coussot, P., Ancey, C., 1999. Rheophysical classification of concentrated suspensions and granular pastes. Phys. Rev. E 59 (4), 4445–4457.
Coussot, P., Laigle, D., Arattano, M., Deganutti, A., Marchi, L., 1998. Direct determination of rheological characteristics of debris flow. J. Hydraul. Eng. 124 (8), 865–868.
Coussot, P., Nguyen, Q.D., Huynh, H.T., Bonn, D., 2002. Avalanche behavior in yield stress fluids. Phys. Rev. Lett. 88 (17), 175501.
Eilertsen, R.S., Hansen, L., Bargel, T.E.H., Solberg, I.-L., 2008. Clay slides in the Malselv valley, northern Norway: characteristics, occurrence, and triggering mechanisms. Geomorphology 93 (3-4), 548–562.
Gattinoni, P., Scesi, L., Arieni, L., Canavesi, M., 2012. The February 2010 large landslide at Maierato, Vibo Valentia, Southern Italy. Landslides 9 (2), 255–261.
Giraud, A., Antoine, P., van Asch, T., Nieyumenhuis, J., 1991. Geotechnical problems caused by glaciolacustrine clays in the French Alps. Eng. Geol. 31, 185–195.
Gomberg, J., Schulz, W., Bodin, P., Kean, J., 2011. Seismic and geodetic signatures of fault slip at the Slumgullion Landslide Natural Laboratory. J. Geophys. Res. 116, B09404.
Huang, X., Garcia, M.H., 1998. A Herschel–Bulkley model for mud flow down a slope. J. Fluid Mech. 374, 305–333.
Iverson, R.M., 2005a. Debris-flow mechanics. In: Jakob, M., Hungr, O. (Eds.), Debris-flow Hazards and Related Phenomena. Springer, Berlin Heidelberg, pp. 105–134.
Iverson, R.M., 2005b. Regulation of landslide motion by dilatancy and pore pressure feedback. J. Geophys. Res. 110.
Iverson, R.M., Reid, M.E., LaHusen, R.G., 1997. Debris-flow mobilization from landslides. Annu. Rev. Earth Planet. Sci. 25, 85–138.
Iverson, R.M., Reid, M.E., Logan, M., LaHusen, R.G., Godt, J.W., Griswold, J.P., 2011. Positive feedback and momentum growth during debris-flow entrainment of wet bed sediment. Nat. Geosci. 4, 116–121.
Jaboyedoff, M., Pedrazzini, A., Loye, A., Opikofer, I., M., G. P., Locat, J., 2009. Earth flow in a complex geological environment: The example of Pont Bourquin, Les Diablerets (Western Switzerland), in: Malet, J.-P., A., R., Bogaard, T. (Eds.), Landslide Processes, From Geomorphologic Mapping to Dynamic Modelling. CERG Ed., Strasbourg, France, pp. 131–137.
Jeong, S.W., 2013. The viscosity of fine-grained sediments: a comparison of low- to medium-activity and high-activity clays. Eng. Geol. 154, 1–5.
Johnson, C.G., Kokelaar, B.P., Iverson, R.M., Logan, M., LaHusen, R.G., Gray, J.M.N.T., 2012. Grain-size segregation and levee formation in geophysical mass flows. J. Geophys. Res. 117, F01032.
Jongmans, D., Bièvre, G., Renalier, F., Schwartz, S., Beaurez, N., Orengo, Y., 2009. Geophysical investigation of a large landslide in glacio-lacustrine clays in the Trièves area (French Alps). Eng. Geol. 109, 45–56.
Khaldoun, A., Moller, P., Fall, A., Wegdam, G., De Leeuw, B., Méheust, Y., Fossum, J.O., Bonn, D., 2009. Quick clay and landslides of clayey soils. Phys. Rev. Lett. 103, 188301.
Larose, E., Roux, P., Campillo, M., 2007. Reconstruction of Rayleigh–Lamb dispersion spectrum based on noise obtained from an air-jet forcing. J. Acoust. Soc. Am. 122, 3437.
Mainsant, G., Jongmans, D., Chambon, G., Larose, E., Baillet, L., 2012a. Shear-wave velocity as an indicator for rheological changes in clay materials: lessons from laboratory experiments. Geophys. Res. Lett. 39, L19301.
Mainsant, G., Larose, E., Bronnimann, C., Jongmans, D., Micoud, C., Jaboyedoff, M., 2012b. Ambient seismic noise monitoring of a clay landslide: toward failure prediction. J. Geophys. Res. 117.
Ovarlez, G., Rodts, S., Chateau, X., Coussot, P., 2009. Phenomenology and physical origin of shear localization and shear banding in complex fluids. Rheol. Acta 48, 831–844.
Park, C.B., Miller, R.D., Xia, J., 1999. Multichannel analysis of surface waves. Geophysics 64, 800–808.
Picarelli, L., Urciuoli, G., Ramondini, M., Comegna, L., 2005. Main features of mudslides in tectonised highly fissured clay shales. Landslides 1, 215–230.
Piccinini, L., Berti, M., Simoni, A., Bernardi, A.R., Ghirotti, M., Gargini, A., 2014. Slope stability and groundwater flow system in the area of Lizzano in Belvedere (Northern Apennines, Italy). Eng. Geol. 183, 276–289.
Quan Luna, B., Remaître, A., van Asch, T.W.J., Malet, J.-P., van Westen, C.J., 2012. Analysis of debris flow behavior with a one dimensional run-out model incorporating entrainment. Eng. Geol. 128, 63–75.
Renalier, F., Bièvre, G., Jongmans, D., Campillo, M., Bard, P.Y., 2010. Clayey landslide investigations using active and massive *Vs* measurements. Advances in Near-Surface Seismology and Ground-Penetrating Radar. No. 15 in Geophys. Dev. Ser, pp. 397–414.
van Asch, T.W.J., Malet, J.P., 2009. Flow-type failures in fine-grained soils: an important aspect in landslide hazard analysis. Nat. Hazards Earth Syst. Sci. 9, 1703–1711.
Viktorov, I., 1967. Rayleigh and Lamb Waves: Physical Theory and Applications. Plenum Press, New York.